



Original Article

# Integrative Characterization of Immune-relevant Genes in Hepatocellular Carcinoma

Wei-Feng Hong<sup>1#</sup>, Yu-Jun Gu<sup>2#</sup>, Na Wang<sup>3#</sup>, Jie Xia<sup>3</sup>, Heng-Yu Zhou<sup>3,4</sup>, Ke Zhan<sup>5</sup>, Ming-Xiang Cheng<sup>6</sup> and Ying Cai<sup>3,7\*</sup> 

<sup>1</sup>Department of Medical Imaging, The First Affiliated Hospital of Guangdong Pharmaceutical University, Guangzhou, Guangdong, China; <sup>2</sup>Department of Ultrasonic Medicine, The First Affiliated Hospital of Sun Yat-Sen University, Guangzhou, Guangdong, China; <sup>3</sup>Key Laboratory of Molecular Biology for Infectious Diseases (Ministry of Education), Institute for Viral Hepatitis, Department of Infectious Diseases, The Second Affiliated Hospital, Chongqing Medical University, Chongqing, China; <sup>4</sup>College of Nursing, Chongqing Medical University, Chongqing, China; <sup>5</sup>Department of Gastroenterology, The Second Affiliated Hospital, Chongqing Medical University, Chongqing, China; <sup>6</sup>Department of Hepatobiliary Surgery, The Second Affiliated Hospital, Chongqing Medical University, Chongqing, China; <sup>7</sup>Department of Intensive Care Medicine, The Second Affiliated Hospital, Chongqing Medical University, Chongqing, China

Received: 27 November 2020 | Revised: 18 February 2021 | Accepted: 21 February 2021 | Published: 8 March 2021

## Abstract

**Background and Aims:** Tumor microenvironment plays an essential role in cancer development and progression. Cancer immunotherapy has become a promising approach for the treatment of hepatocellular carcinoma (HCC). We aimed to analyze the HCC immune microenvironment characteristics to identify immune-related genetic changes. **Methods:** Key immune-relevant genes (KIRGs) were obtained through integrating the differentially expressed genes of The Cancer Genome Atlas, immune genes from the Immunology Database and Analysis Portal, and immune differentially expressed genes determined by single-sample gene set enrichment analysis scores. Cox regression analysis was performed to mine therapeutic target genes. A regulatory network based on KIRGs, transcription factors, and immune-related long non-coding RNAs (IRLncRNAs) was also generated. The outcomes of risk score model were validated in a testing cohort and in clinical samples using tissue immunohistochemistry staining. Correlation analysis

between risk score and immune checkpoint genes and immune cell infiltration were investigated. **Results:** In total, we identified 21 KIRGs, including programmed cell death-1 (PD-1) and cytotoxic T-lymphocyte associated protein 4 (CTLA4), and found IKBKE, IL2RG, EDNRA, and IGHA1 may be equally important to PD-1 or CTLA4. Meanwhile, KIRGs, various transcription factors, and IRLncRNAs were integrated to reveal that the NRF1-AC127024.5-IBKKE axis might be involved in tumor immunity regulation. Furthermore, the immune-related risk score model was established according to KIRGs and key IRLncRNAs, and verified more obvious discriminating power in the testing cohort. Correlation analysis indicated *TNFSF4*, *LGALS9*, *KIAA1429*, *IDO2*, and *CD276* were closely related to the risk score, and CD4 T cells, macrophages, and neutrophils were the primary immune infiltration cell types. **Conclusions:** Our results highlight the importance of immune genes in the HCC microenvironment and further unravel the underlying molecular mechanisms in the development of HCC.

**Citation of this article:** Hong WF, Gu YJ, Wang N, Xia J, Zhou HY, Zhan K, et al. Integrative characterization of immune-relevant genes in hepatocellular carcinoma. J Clin Transl Hepatol 2021;9(3):301–314. doi: 10.14218/JCTH.2020.00132.

**Keywords:** Hepatocellular carcinoma; Immune gene; Immunotherapy; Tumor microenvironment; Risk model.

**Abbreviations:** CTLA4, cytotoxic T-lymphocyte associated protein 4; DEGs, differentially expressed genes; DETFs, differentially expressed transcription factors; GSEA, gene set enrichment analysis; HCC, hepatocellular carcinoma; IDEGs, immune differentially expressed genes; IGs, immune genes; IKBKE, inhibitor of nuclear factor kappa-B kinase subunit epsilon; ImmPort, Immunology Database and Analysis Portal; IRG, immune-relevant gene; IRLncRNAs, immune-related long non-coding RNAs; KEGG, Kyoto Encyclopedia of Genes and Genomes; KIRGs, key immune-relevant genes; Lasso, least absolute shrinkage and selection operator; LIHC, liver hepatocellular carcinoma; PD-1, programmed cell death-1; ROC, receiver operating characteristic; ssGSEA, single sample gene set enrichment analysis; STRING, search tool for the retrieval of interacting genes/proteins database; TCGA, The Cancer Genome Atlas; TIMER, tumor immune estimation resource; WGCNA, weighted gene co-expression networks analysis.

<sup>#</sup>These authors contributed equally to this study.

\***Correspondence to:** Ying Cai, Key Laboratory of Molecular Biology for Infectious Diseases (Ministry of Education), Institute for Viral Hepatitis, Department of Infectious Diseases; Department of Intensive Care Medicine, The Second Affiliated Hospital, Chongqing Medical University, 1<sup>#</sup> Yixueyuan Road, Yuzhong District, Chongqing 400000, China. ORCID: <https://orcid.org/0000-0002-1782-719X>. Tel: +86-15923330181, E-mail: caiying@cqmu.edu.cn

## Introduction

Liver cancer is the most common malignancy and the fourth leading cause of cancer-related mortality worldwide.<sup>1</sup> Hepatocellular carcinoma (HCC), a predominant type of primary liver cancer, has become a major public health problem. Although surgical resection is a potentially curative modality for a minority of early-stage HCC patients,<sup>2</sup> as many as 70% of these patients will experience disease recurrence within 5 years.<sup>3</sup> Due to the occult onset of HCC, most advanced patients are not eligible for the timely administration of effective treatment.<sup>4</sup> Sorafenib, as a multi-kinase

inhibitor, has been approved by the Food and Drug Administration and recommended as the first-line treatment in this population based on the "SHARP" trial, with median overall survival of 6.5 months.<sup>2,5,6</sup> Then, the "REFLECT" trial demonstrated that lenvatinib was non-inferior to sorafenib for overall survival in untreated advanced HCC patients.<sup>7</sup> It only showed some clinical benefits for secondary endpoints in progression-free survival, time to progression, and objective response rate. The current status of HCC recurrence and metastasis are not optimistic; therefore, novel and effective treatment options are desperately in need of further exploration to decrease recurrence rates.

Increasing evidence has shown that the tumor microenvironment plays an essential role in cancer development and progression. With improved understanding of biological interactions within the tumor microenvironment, immune system and tumor cells, cancer immunotherapy has appeared to provide tremendous promise as a cancer treatment modality in recent years. Typically, in the liver, large quantities of innate and adaptive immune cells play a critical role in immune surveillance to detect and eliminate pathogens and participate in immune response and regulation of host defenses.<sup>8</sup> However, the inflammatory state, due to risk factors that contribute to HCC, such as chronic infection with hepatitis B virus or hepatitis C virus, will change the tumor microenvironment and facilitate evasion of immune surveillance, leading to tumor tolerance and promoting the development of HCC.<sup>8</sup> Hence, targeted immunotherapy is actively researched with the goal of inhibiting aberrant oncogenic pathways and improving prognosis.

At present, immune checkpoint inhibitors are considered one of the immunotherapies for rapid development to promote immune reconstitution and restore immune cell function.<sup>9</sup> Programmed cell death-1 (PD-1) and cytotoxic T-lymphocyte associated protein 4 (CTLA4) blockage therapies have become promising approaches for the treatment of HCC.<sup>10-13</sup> Unfortunately, in some studies, overall survival and improved recurrence-free survival did not achieve the pre-defined statistical significance criteria.<sup>14</sup> It has been suggested that the HCC microenvironment can form a potent immune tolerance system, which greatly hinders the efficacy of immune checkpoint therapy. Therefore, remodeling the immune tolerant microenvironment of HCC could be of great significance for HCC immunotherapy.

Given the complexity of immunotherapy and tumor heterogeneity, extensive genomic analysis could provide clinical options, including personalized therapies for patients with cancer. We systematically integrated genomic profiling to illustrate the global portrait of the HCC immune microenvironment characteristics to further identify the immune-related genetic changes. In addition, immune-related models and networks were also established to shed light on the potential mechanism of immune therapeutic targets.

## Methods

### Datasets acquisition and pre-processing

Fragments per kilobase million upper quartile RNA-Seq gene expression profile of liver hepatocellular carcinoma (LIHC) were downloaded from The Cancer Genome Atlas (TCGA) (<https://portal.gdc.cancer.gov/>), including 50 normal tissue and 374 primary tumor samples.<sup>15</sup> A list of 1,811 immune genes (IGs), including 17 immune categories according to different molecular function, were obtained from the Immunology Database and Analysis Portal (ImmPort) (<https://www.immport.org/home>)<sup>16</sup> after eliminating reiterated genes. One of the major collections (C7: immunologic signatures) in the molecular signatures database

(MSigDB) of Gene Set Enrichment Analysis (GSEA) (<https://www.gsea-msigdb.org/gsea/index.jsp>)<sup>17</sup> is a collection of 4,872 annotated gene sets that represent cell types, states, and perturbations within the immune system.<sup>18</sup> The immunologic gene sets and 28 immune signaling pathways were also collected and processed for subsequent analyses. The data of tumor immune infiltration in TCGA-LIHC was downloaded from the tumor immune estimation resource (known as TIMER) (<https://cistrome.shinyapps.io/timer/>).<sup>19</sup>

### Screening immune-relevant genes (IRGs)

To evaluate the enrichment scores of every sample on each immune-related term in RNA-Seq data of TCGA-LIHC, single-sample gene set enrichment analysis (ssGSEA) was used to generate ssGSEA-score<sup>20</sup> implemented in the R package "GSVA" and "GSEABase". Each score was corrected between 0 and 1. Patients were divided into a high-immune score (Immunity\_H) and a low-immune score (Immunity\_L) group using unsupervised hierarchical clustering of R package "sparcl".

Differentially expressed gene (DEG) analysis was performed via the R package "Limma" based on the empirical Bayes method.<sup>21</sup> Immune differentially expressed genes (IDEGs) were determined by Immunity\_H to Immunity\_L ratio, with cutoff criteria of absolute log<sub>2</sub> fold-change ( $|\log_2 FC|$ ) >1.0 and false discovery rate <0.05. Significant DEGs of RNA-Seq data from TCGA-LIHC project were also identified by the same approach. Then, overlapping DEGs, IDEGs, and IGs were assessed and provided 77 interacting genes as the IRGs in the present study.

### Construction of weighted gene co-expression networks and identification of key IRGs

Based on the expression of 77 IRGs with complete clinical data in tumor tissues from TCGA-LIHC project, weighted gene co-expression networks analysis (WGCNA) was carried out to create expression modules and analyze the correlation of each module with immune traits (ImmuneGroup, StromalScore, ImmuneScore, ESTIMATEScore, and TumorPurity) using the R package WGCNA by hierarchical clustering of adjacency-based dissimilarity.<sup>22</sup> Module eigengenes were defined as the first principle component of each gene module and regarded as representative of genes in each module. Gene significance was calculated to measure the Pearson correlation between gene expression and sample traits and to identify the significance of each module. We selected higher gene significance and defined survival-related modules according to  $p \leq 0.001$  for further analysis. A scale-free topology fit index (scale-free  $R^2$ ) >0.95 was implemented to verify the soft threshold power and maintain optimal mean connectivity. A dynamic hybrid cut method, using a bottom-up algorithm, was applied to identify crucial modules, with cut height-off of 0.25. At last, key immune-relevant genes (KIRGs) in crucial modules were selected by those with module membership >0.5. General characteristics of KIRGs were analyzed using GSCALite (<http://bioinfo.life.hust.edu.cn/web/GSCALite/>).<sup>23</sup>

### Construction of co-expression network based on KIRGs

To analyze the function of KIRGs, the relationship between transcription factors and KIRGs was explored. The transcription factors set was extracted from the Cistrome Project (<http://www.cistrome.org/>)<sup>24</sup> and subjected to expression

differential analysis by the R package "Limma", with cut-off value of  $|\log_{2}FC| > 1.0$  and adjusted  $p$ -value of  $< 0.05$ . The significant correlations between the differentially expressed transcription factors (DETFs) and KIRGs (DETFs-KIRGs) were calculated by Pearson's test, with  $p$ -value of  $< 0.0001$  and correlation coefficient of  $> 0.30$ , which was visualized by Cytoscape software (3.7.1) in the appropriate type of correlation network.

Meanwhile, considering immune-related long non-coding RNAs (lncRNAs) involved in the mRNA transcript process of KIRGs, the network of lncRNAs-KIRGs was established using the co-expression analysis approach as described above. The profile of long non-coding RNAs was taken from the annotation data of TCGA-LIHC. Subsequently, the network of DETFs and lncRNAs (DETFs-lncRNAs) was also generated (correlation coefficient  $> 0.30$  and  $p < 0.0001$ ). Finally, the DETFs-lncRNA-KIRGs regulatory network was integrated for the pairs of the above three networks' data.

### **Risk score model construction and verification**

TCGA-LIHC patients were randomly divided at the ratio of 1:1 into two cohorts (training cohort and testing cohort). To avoid overfitting, least absolute shrinkage and selection operator (Lasso) Cox regression was applied to eliminate genes generated from univariate Cox analysis of all genes of lncRNAs-KIRGs. Then, we performed multivariate Cox regression to construct a risk score model, and the performance was evaluated in the testing cohort. Kaplan-Meier survival analysis and time-dependent receiver operating characteristic (commonly known as ROC) analysis were used to compare the survival states and evaluate the accuracy of the risk score model.

### **Enrichment analysis and protein-protein interaction**

To determine the function and potential regulatory pathways of identified genes, GSEA was explored for biological functions and pathways using the R package "clusterprofiler" and "GSVA", with adjusted  $p$ -value of  $< 0.05$  and  $q$ -value of  $< 0.05$ , as each was regarded as statistically significant. Gene Ontology analysis and Kyoto Encyclopedia of Genes and Genomes (KEGG) pathway enrichment analysis were performed by the web tool "Metascape" (<http://metascape.org/>).<sup>25</sup> The search tool for the retrieval of interacting genes/proteins database (commonly known as STRING) was utilized to assess protein-protein interactions, with information minimum required interaction score: medium confidence (0.40) ([www.string-db.org/](http://www.string-db.org/)).<sup>26</sup>

### **Experimental section**

Paired tumor and peritumor tissues were obtained from patients diagnosed with HCC and who had undergone surgery at the Department of Hepatological Surgery of the Second Affiliated Hospital of Chongqing Medical University (Chongqing, China). All experiments were performed in accordance with the Declaration of Helsinki of the World Medical Association and were approved by the ethics committee of the Second Affiliated Hospital of Chongqing Medical University (No. 2020-004). All participants provided written informed consent.

Tissue proteins were lysed using radio immunoprecipitation assay lysis buffer (CWBIO, Beijing, China) with protease inhibitor cocktail (CWBIO). Protein concentration was measured with a bicinchoninic acid assay (CWBIO). The same amount of total proteins was subjected to SDS-PAGE, followed by a standard western blotting procedure with the

primary antibodies and secondary antibodies (Supplementary Table 1), and detection using an enhanced chemiluminescence system (Advansta, Menlo Park, CA, USA).

Tissue paraffin sections were prepared for immunohistochemistry staining, according to standard procedures. The slides were visualized using 3,3'-diaminobenzidine substrate kit (Abcam, Cambridge, UK) and counterstained with hematoxylin (Solarbio, Beijing, China). Stained slides were scanned by the Motic Easyscanner (Motic, Hong Kong, China) and the images were captured with Motic DS Assistant Lite (Motic VM V1 Viewer 2.0).

Tissue total RNA was extracted using TRIzol reagent (Invitrogen, Carlsbad, CA, USA), following the manufacturer's instructions. The cDNA library was constructed by reverse transcription using a commercial reverse-transcription kit (Takara, Shiga, Japan) according to the manufacturer's protocol. The cDNA was amplified using SYBR Green Master Mix (Bimake, Houston, TX, USA) and normalized by GAPDH. Quantitative polymerase chain reaction primers (Supplementary Table 2) were synthesized by Invitrogen.

### **Statistical analysis**

All statistical analyses were performed in R version 3.6.0 and GraphPad Prism software 8.0, and  $p$ -values  $< 0.05$  were considered significant. Continuous variables, such as difference analysis, were performed by  $t$ -test or Wilcoxon's test, according to the normality of data distribution. Correlation analysis of categorical variables was carried out with the chi-squared test. Correlations between continuous variables were estimated using the Pearson correlation, while Spearman's correlation was used to assess the association between non-normally distributed data.

## **Results**

### **Initial screening IRGs**

To screen significant immune biomarkers, we incorporated important databases in the initial workflow (Fig. 1A). A total of 7,667 DEGs were identified from TCGA-LIHC dataset (Supplementary Fig. 1A, B). To understand each tumor sample's immune status, the corresponding enrichment scores on every immune-related term were calculated based on the ssGSEA method. By unsupervised hierarchical clustering, patients were clustered into the Immunity\_H group ( $n=170$ ) and the Immunity\_L group ( $n=204$ ) (Supplementary Fig. 1C). Stromal cells and immune cells were the non-tumor components of the immune microenvironment which reflected tumor immune infiltration and tumor purity. The stromal scores and immune scores were calculated and combined to estimate scores in order to display tumor purity by the ESTIMATE algorithm (Fig. 2A; Supplementary Table 3). Upon comparison with the Immunity\_L group, stromal scores, immune scores, and ESTIMATE scores were significantly higher in the Immunity\_H group, while the lower level of tumor purity represented the low activity of tumor cells ( $p < 0.001$ ) (Fig. 2B-E). Then, enrichment analysis of biological functions and pathways in the two groups was performed using GSEA. The Immunity\_H group was identified when the enrichment score was  $> 0$ , and found to be mainly enriched in complement activation (classical pathway), humoral immune response mediated by circulating immunoglobulin and MHC class II protein complex in the aspect of biological function (Fig. 2F). Allograft rejection, intestinal immune network for IgA production, and primary immunodeficiency embodied the pathway

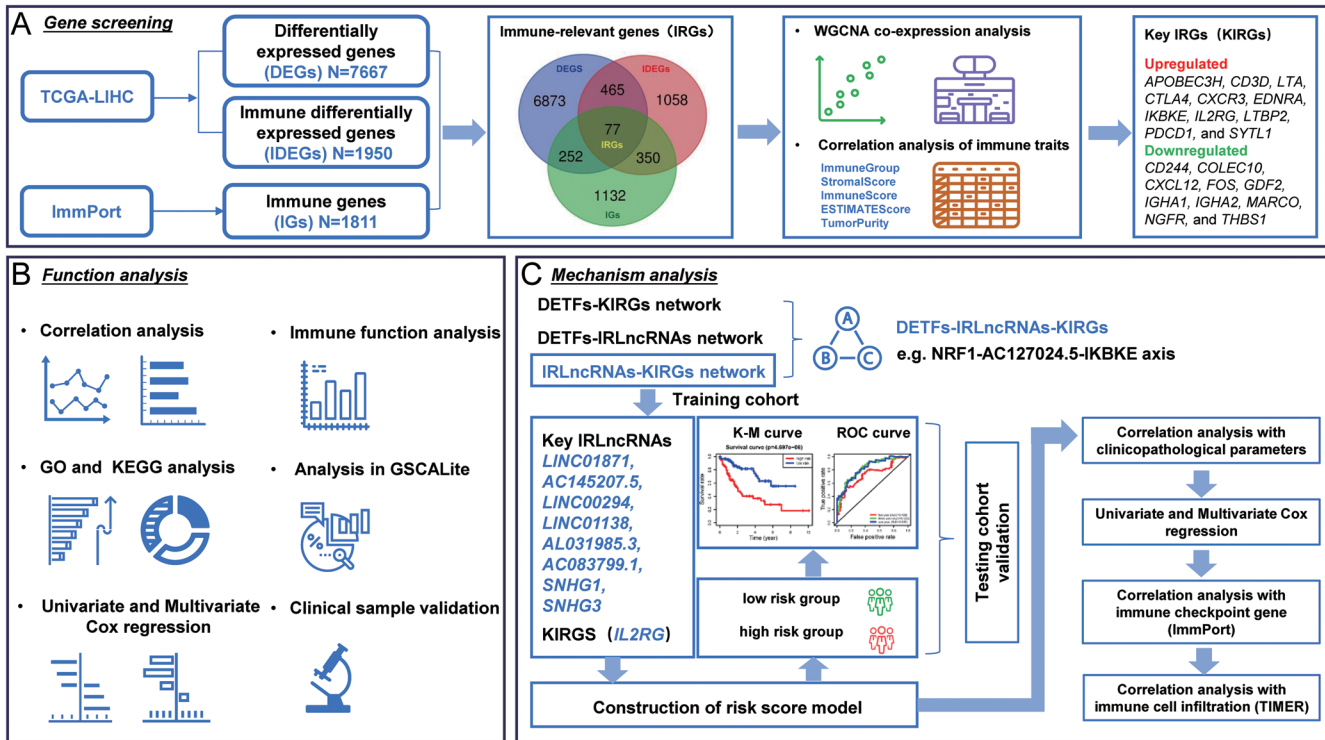


**Fig. 1. Flow chart of immune-relevant gene screening, function analysis, and mechanism analysis.** (A) Screening for KIRGs incorporated from TCGA and ImmPort. (B) Schematic diagram for function analysis of KIRGs. (C) Flow chart for underlying mechanism analysis of KIRGs combined with transcription factors and lncRNAs.

enrichment results (Fig. 2G). Next, the bubble chart showed the top 10 biological functions in the Immunity\_H group and the Immunity\_L group (Fig. 2H). Enrichment analysis of the pathway only focused on the Immunity\_H group (Supplementary Table 4). Meanwhile, 1,950 IDEGs were obtained by differential analysis for the Immunity\_H and Immunity\_L groups (Supplementary Fig. 1D, E). Finally, 77 IRGs were screened out by overlapping the DEGs, IDEGs, and IGs in this present study. Gene Ontology analysis and KEGG pathway enrichment analysis results were statistically confirmed via Metascape (Supplementary Fig. 1F, G).

**Identification of the modules associated with immune traits by construction of WGCNA**

WGCNA was applied to find important modules most associated with immune traits based on 77 IRGs. A total of seven modules were identified by setting soft threshold power and cut height-off value. IRGs in the gray module were identified as non-clustering genes (Fig. 3A, B). In the heatmap of module-trait relationships, the blue module (12 IRGs) and brown module (9 IRGs) manifested significant correlation of immune traits, especially by ImmuneScore (correlation coefficient of 0.73,  $p=4e-64$ ) and StromalScore (correlation coefficient of 0.65,  $p=7e-47$ ), respectively. Genes in these two modules with module membership of  $>0.5$  were defined as KIRGs (Fig. 3C).

**Functional analysis of the KIRGs signature**

We analyzed the fundamental functional of the KIRGs (Fig.

1B). Differential analysis of KIRGs' expressions was performed, with 11 genes (*APOBEC3H*, *CD3D*, *CTLA4*, *CXCR3*, *EDNRA*, *inhibitor of nuclear factor kappa-B kinase subunit epsilon* (*IKBKE*), *IL2RG*, *LTA*, *LTBP2*, *PDCD1*, and *SYTL1*) showing high expression and 9 genes (*CD244*, *COLEC10*, *CXCL12*, *FOS*, *GDF2*, *IGHA1*, *IGHA2*, *MARCO*, *NGFR*, and *THBS1*) showing low expression in tumor tissue ( $p<0.05$ ) (Fig. 4A). Correlation analysis of 21 KIRGs showed that *CXCR3* was highly associated with *CD3D* and *LTA* (correlation coefficient of  $>0.80$ ,  $p<0.05$ ) (Fig. 4B). To display interactive relationships among proteins of KIRGs, a protein-protein interaction network was constructed by the STRING database. *LTA*, *CTLA4*, *FOS*, and *CXCL12* had the most interactive lines ( $n>10$ ) in the bar graph, which totaled 60 lines (Fig. 4C, D). High node degrees could indicate an essential role in tumor immune processes.

Gene Ontology analysis and KEGG pathway enrichment analysis were performed using the R package "clusterprofiles". To demonstrate more information from the results, the top 20 Gene Ontology terms were enriched as a Gene Ontology heatmap, mainly in "leukocyte migration" and "humoral immune response" (Fig. 4E). We also found that the three terms of "response to oxygen levels", "response to hypoxia" and "response to decreased oxygen levels" enriched from the same genes (Fig. 4E). In the KEGG circle map, KIRGs were enriched in some common and critical pathways referring to tumorigenesis and progression, such as "T cell receptor signaling pathway", "Cytokine-cytokine receptor interaction" and "PI3K-Akt signaling pathway" and so on (Fig. 4F).

To further verify whether KIRGs were closely related to immune function, 29 terms from the ImmPort database served as the candidate profile and a gene set including 21 KIRGs was found to be enriched in eight immune

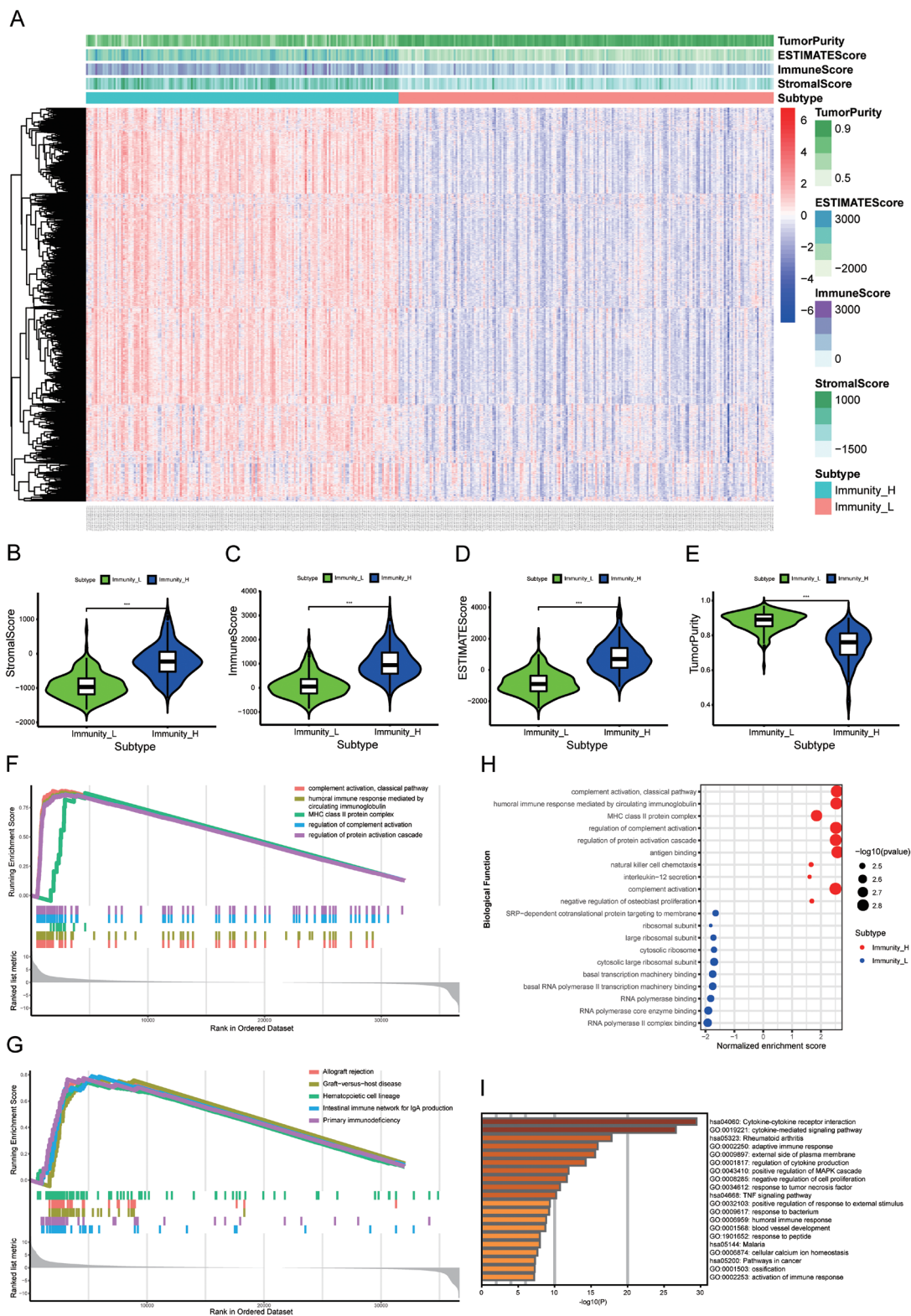


**Fig. 2. Microenvironment signatures of TCGA-LIHC cohort and enrichment analysis.** (A) Heatmaps showed expression profiles for microenvironment signatures of stromal scores, immune scores, ESTIMATE scores, and tumor purity with unsupervised hierarchical clustering analyses. (B–E) Stromal scores, immune scores, ESTIMATE scores and tumor purity in the Immunity\_H group and the Immunity\_L group. (\*\* $p < 0.001$ ) (F–G) Enrichment analysis of biological functions and pathways in the Immunity\_H group (top 5). (H) Bubble chart of top 10 biological functions in the Immunity\_H and Immunity\_L groups. (I) Heatmap of Gene Ontology and KEGG enrichment analysis for IRGs via Metascape.

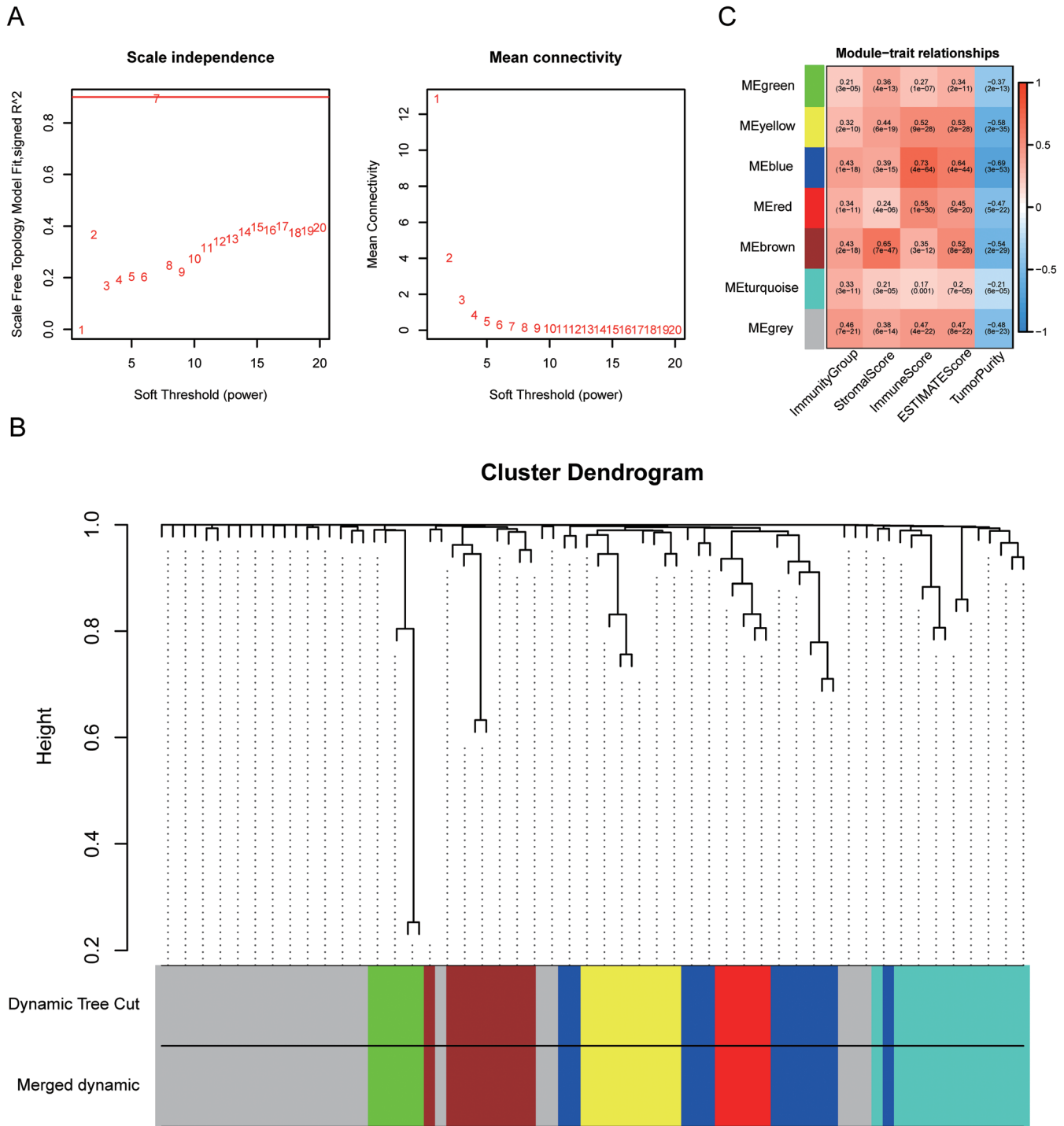


**Fig. 3. Construction of WGCNA co-expression modules and identification of modules associated with immune traits.** (A) Analyses of the scale-free topology fit index of the soft threshold power (left panel) and the mean connectivity of soft threshold power (right panel). (B) A cluster dendrogram of 77 IRGs with various modules constructed by hierarchical clustering of adjacency-based dissimilarity; different colors represent different modules. (C) Heatmap of relationships between module eigengenes and immune trait.

terms, namely Check-point, Th1 cells, Tfh, T cell coinhibition, plasmacytoid dendritic cells, CCR, TIL, and regulatory T cells, based on the ssGSEA-score of the R package "GSVA" (Supplementary Fig. 2A-C). Next, we extracted all the genes of some critical immune terms from TCGA-

LIHC project and differential analysis of expression was implemented between the Immunity\_H group and the Immunity\_L group (Supplementary Fig. 3A-E). Besides, due to multiple filters, *IKBKE*, *IL2RG*, *EDNRA*, and *IGHA1* were screened out more significantly with  $p < 0.2$  using



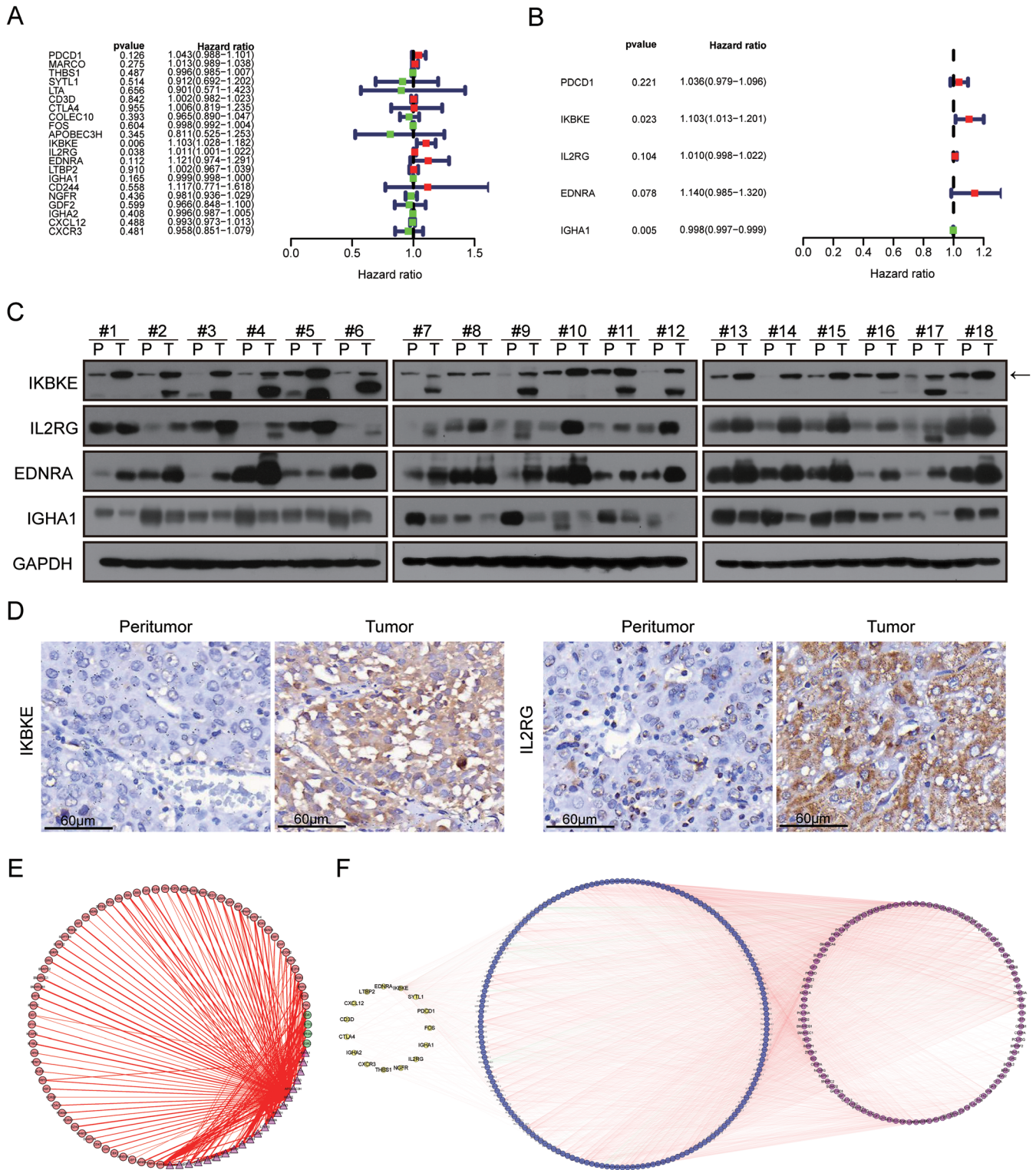


**Fig. 5. Cox regression of 21 KIRGs and construction of regulatory networks.** (A) Univariate Cox regression. (B) Multivariate Cox regression. (C) Western blot of protein expression in HCC and paired peritumor tissues from 18 patients. (D) Immunohistochemical staining of the representative KIRGs IKBKE and IL2RG in HCC and paired peritumor tissues. (E) Construction of DETFs-KIRGs networks. (F) Construction of DETFs-IRLncRNAs-KIRGs regulatory networks.

Of the 21 KIRGs, the vast majority of variants occurred as single nucleotide polymorphisms and missense muta-

tions in the included samples (Supplementary Fig. 4A, B). The top 10 frequently mutated genes were *GDF2*, *LTBP2*,

*THBS1*, *CXCR3*, *EDNRA*, *MARCO*, *NGFR*, *CD244*, *FOS* and *APOBEC3H*, with 91.18% alteration in at least one sample (Supplementary Fig. 4C, E). *GDF2*, *LTBP2*, and *THBS1* alterations were observed in 15% of tumors; *NGFR* had multiple alterations of missense mutation, splice site, and frame shift deletion (Supplementary Fig. 4E). C > T and C > A accounted for most of the single nucleotide mutation types (Supplementary Fig. 4D). Meanwhile, we noted that somatic copy number alterations occurred more often in heterozygous copy number variations than in homozygous ones (Supplementary Fig. 4F). *IKBKE*, *COLEG10*, and *CD244* manifested mainly in the statistical processing of heterozygous amplifications (Supplementary Fig. 4F).

Further, differential methylation between tumor and paired normal tissues were found, along with that of other tumor types (Supplementary Fig. 4G). *PDCD1*, *CTLA4*, and *MARCO* indicated high levels of methylation in HCC tissues, while *CXCL12* and *EDNRA* showed a high level in paired normal tissues. We also observed the relationships between methylation levels and corresponding gene expression, which displayed that *PDCD1* methylation had a positive correlation with expression, whereas *IKBKE* and *EDNRA* methylation showed negative relationships in most tumors (Supplementary Fig. 4H).

We also investigated the difference of gene expression between pathway activity groups (activation and inhibition). These KIRGs were also involved in apoptosis, cell cycle, DNA damage response, epithelial to mesenchymal transition, and the RAS/MAPK biological process (Supplementary Fig. 4I). *PDL1*, *CTLA4*, *IKBKE*, and *IL2RG* could promote apoptosis and activate DNA damage response and epithelial to mesenchymal transition (Supplementary Fig. 4J). Eventually, drug sensitivity analysis was performed for 21 KIRGs of HCC lines in the Genomics of Drug Sensitivity in Cancer<sup>27</sup> and Cancer Therapeutics Response Portal<sup>28</sup> databases by Spearman correlation analysis with small molecule/drug sensitivity (Supplementary Fig. 5 and 6).

### Construction of the DTFs-IRLncRNA-KIRGs network

Subsequently, in order to observe transcription factors involved in the regulation of KIRGs, the correlations of KIRGs to DTFs were generated according to co-expression analysis and visualized as a regulatory network (Fig. 1C). A total of 162 positive correlation pairs of DTFs-KIRGs were found; among these, the pairs of *FOS*-*ERG1* (correlation coefficient of 0.63,  $p=5.2E-43$ ), *CIITA*-*CTLA4* (correlation coefficient of 0.62,  $p=6.3E-43$ ) and *CXCR3*-*CIITA* (correlation coefficient of 0.62,  $p=9.1E-43$ ) showed very high correlation (Fig. 5E). Similarly, the IRLncRNAs-KIRGs network and DTFs-IRLncRNAs network were also constructed. Eventually, combining the three networks, the DTFs-IRLncRNAs-KIRGs regulatory network was built, comprised of 103 DTFs, 175 LncRNAs, and 15 KIRGs, to elucidate underlying regulatory mechanisms (Fig. 5F). Most of the pairs represented positive correlations within the network.

*IKBKE*, having a prominent role among the KIRGs, was related to numerous IRLncRNAs, most obviously *AC127024.5*. Interestingly, in the network, *NRF1* was regarded as the most relevant transcription factor to *AC127024.5* (correlation coefficient of 0.63,  $p=4.94E-43$ ), which indicated that the *NRF1*-*AC127024.5*-*IKBKE* axis might be involved in regulating many biological processes. We also explored the *NRF1*-*AC127024.5*-*IKBKE* axis for immune cell infiltration in TCGA-LIHC patients from the TIMER database, and found an involvement in the vast majority of immune cell infiltration processes, especially those related to B cells, CD4 T cells, neutrophils and macrophages ( $p<0.01$ ) (Supplementary Fig. 7).

Furthermore, univariate and Lasso Cox regressions were implemented to optimize the parameters for screening risk genes among the KIRGs and IRLncRNAs (Fig. 6A, B). In total, *IL2RG* and eight key IRLncRNAs (*LINC01871*, *AC145207.5*, *LINC00294*, *LINC01138*, *AL031985.3*, *AC083799.1*, *SNHG1*, and *SNHG3*) were obtained by multivariate Cox regression in the training cohort. The risk score model was constructed and verified the performance in the testing cohort. Patients in each cohort were divided into a low risk group and a high risk group, according to the median risk score of the training cohort. Survival status, risk scores, and expression patterns of each patient were reflected in Fig. 6C and 6D.

Kaplan-Meier curve analysis showed that the low risk group had a significantly better prognosis than that of the high risk group in the training cohort ( $p=4.70E-06$ ) and the testing cohort ( $p=4.70E-05$ ), respectively (Fig. 6E, G). Time-dependent ROC curve analysis of the risk score model in the training and testing cohorts all determined good predictive accuracy with area under the curve values of 0.826 and 0.724 for 1-year survival, and 0.822 and 0.736 for 3-year survival, respectively (Fig. 6F, H). Therefore, it appeared that the risk score model successfully stratified HCC from TCGA.

In addition, we found that the risk score model was associated with clinicopathological parameters, such as tumor-stage, clinical stage, and survival state by chi-squared test ( $p<0.01$ ) (Fig. 7A). Further analysis of univariate and multivariate Cox regression revealed that risk score could be an independent prognostic indicator for HCC patients ( $p<0.001$ ) (Fig. 7B, C). Representative markers (*IL2RG*, *SNHG1*, *SNHG3*, and *LINC01138*) showed obvious high expression in HCC samples at the mRNA level (Fig. 7D). Meanwhile, the forecast performance of the risk score model was superior to those models based on tumor-stage, node-stage, metastasis-stage, grade, American Joint Committee on Cancer stage, KIRGs and key IRLncRNAs (Supplementary Fig. 8A–G). The multiplex model seemed a dependable indicator for predicting the prognosis of HCC patients.

We analyzed the expression of each immune checkpoint gene of ImmPort for correlation with the integration of risk score resulting from the two cohorts. Pearson's correlation indicated *TNFSF4*, *LGALS9*, *KIAA1429*, *IDO2*, and *CD276* were closely related to risk score ( $p<0.05$ ), shown as a circle map (Fig. 8A). Ultimately, we investigated the measurement of the integrated risk score for immune cell infiltration in TCGA-LIHC patients from the TIMER database and observed that effects of risk score appeared to be concentrated among the CD4 T cells, macrophages, and neutrophils ( $p<0.05$ ), while the B cells, CD8 T cells and dendritic cells did not show significant correlation (Fig. 8B–G).

### Discussion

Rapidly emerged immunotherapy has demonstrated increasing promise in the application of treatment for human cancers. On account of tumor complexity and heterogeneity, only a minority of patients could have benefitted from immunotherapy. Interestingly, the tumor immune microenvironment is closely related to patients' responsiveness after receiving the therapy of immune-checkpoint blockade.<sup>29</sup> Thus, understanding the tumor immune microenvironment's diversity will likely uncover novel biomarkers and provide effective therapeutic targets.

According to the natural and fundamental immunological properties of the liver and the current dilemma of immunotherapy for HCC, in this study, we systematically identified 21 KIRGs that potentially participate in HCC pathogenesis and progression. To obtain more robust and reliable IGs, our results were analyzed by more comprehensive and

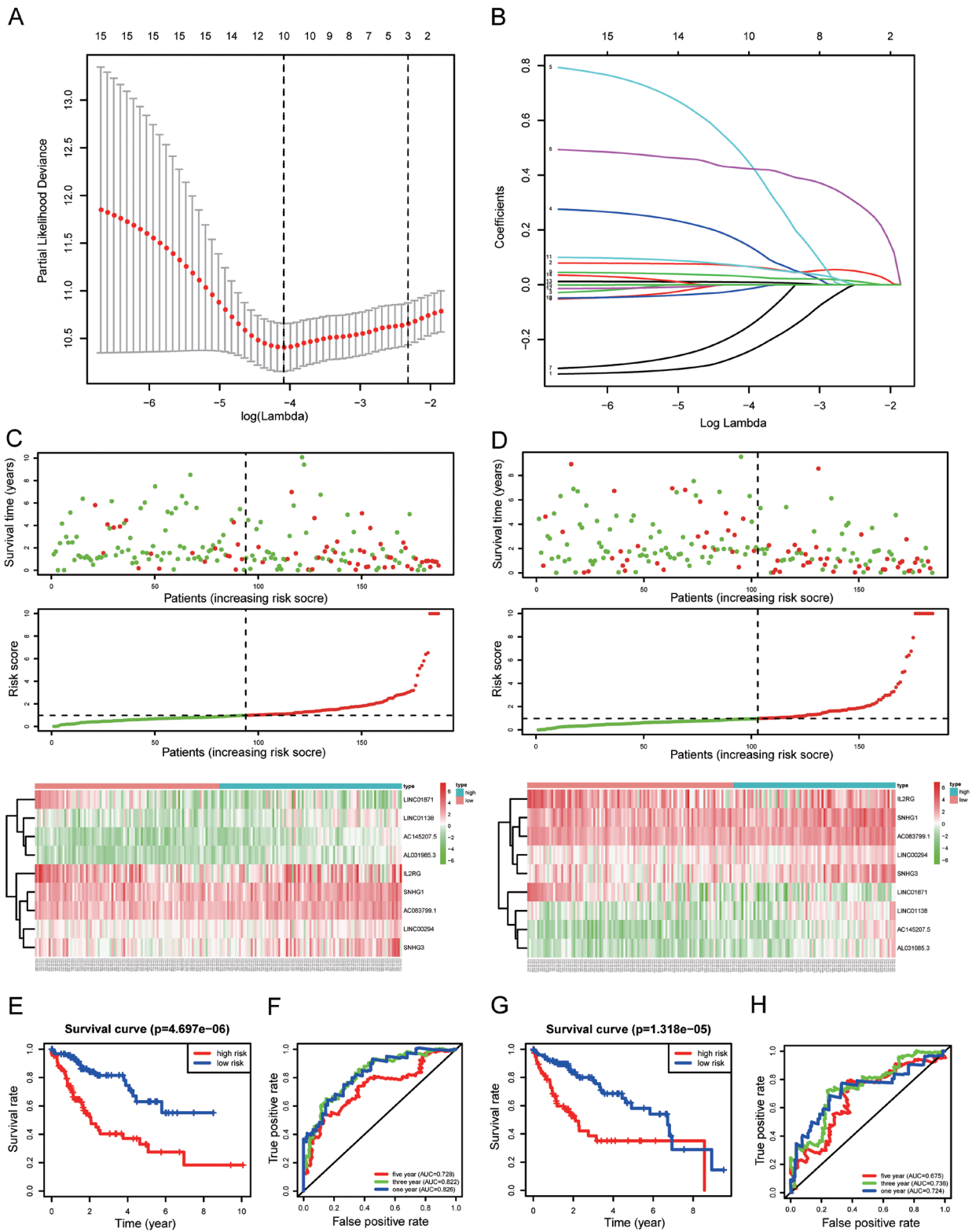


**Fig. 6. Construction of risk score model based on DETFs-IRLncRNAs-KIRGs network.** (A-B) KIRGs and IRLncRNAs were narrowed down by the Lasso algorithm. (C) Survival status scatter plots, risk score distribution, and expression patterns in the training cohort. (D) Survival status scatter plots, risk score distribution, and expression patterns in the testing cohort. (\*\*\*)  $p < 0.001$ . (E) Kaplan-Meier curve analysis of the high risk and low risk groups in the training cohort. (F) Time-dependent ROC curve analysis of the risk score model in the training cohort. (G) Kaplan-Meier curve analysis of the high risk and low risk groups in the testing cohort. (H) Time-dependent ROC curve analysis of the risk score model in the testing cohort.

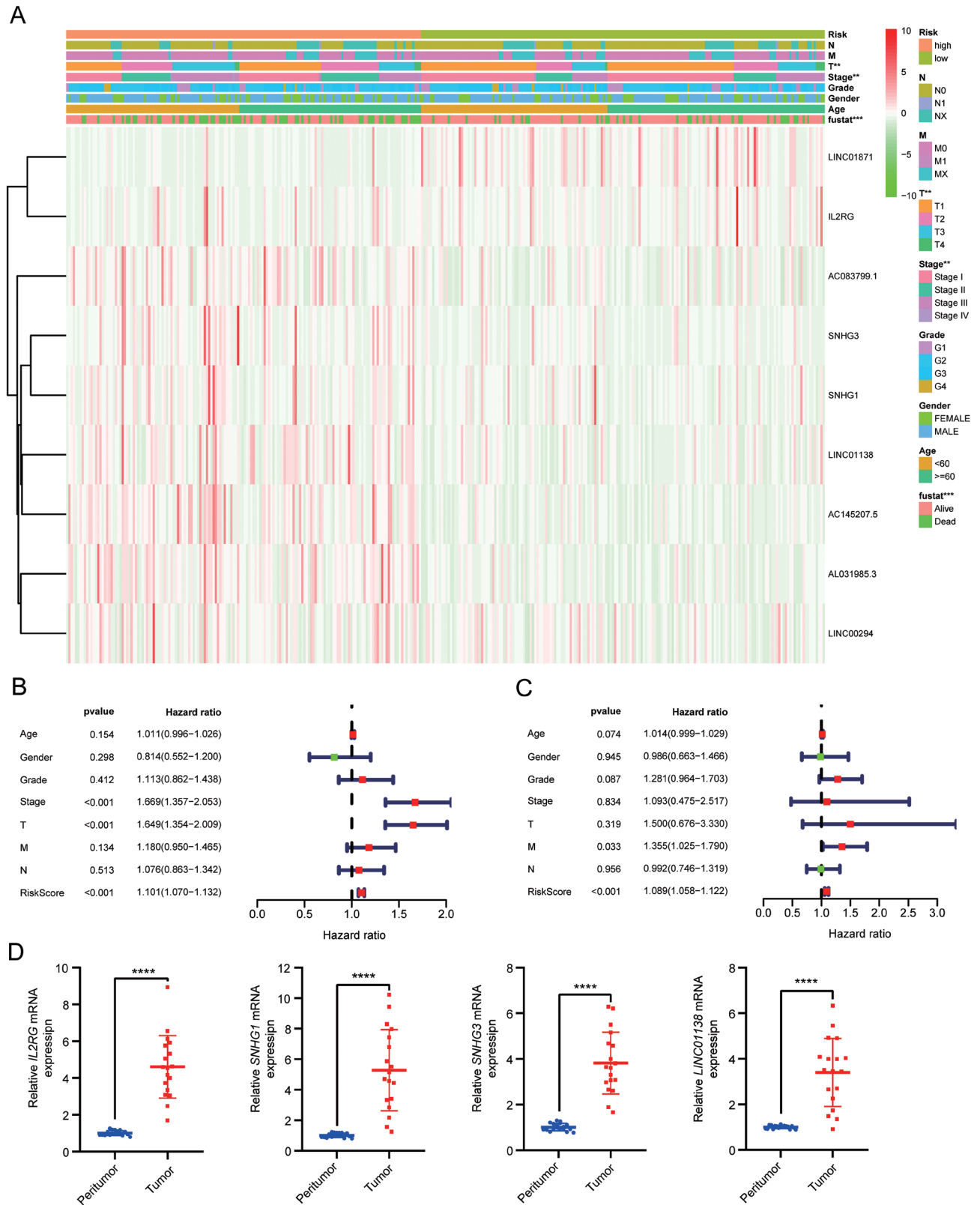


**Fig. 7. Relationship between risk score model and clinicopathological parameters.** (A) Expression profiles of risk genes and association with clinicopathological characteristics. (B–C) Univariate and multivariate Cox regression analyses of risk score and clinicopathological characteristics. (D) Representative key lncRNAs were detected by real-time polymerase chain reaction of HCC and paired peritumor tissues from 18 patients. Abbreviations: M, metastasis; N, node; T, tumor.

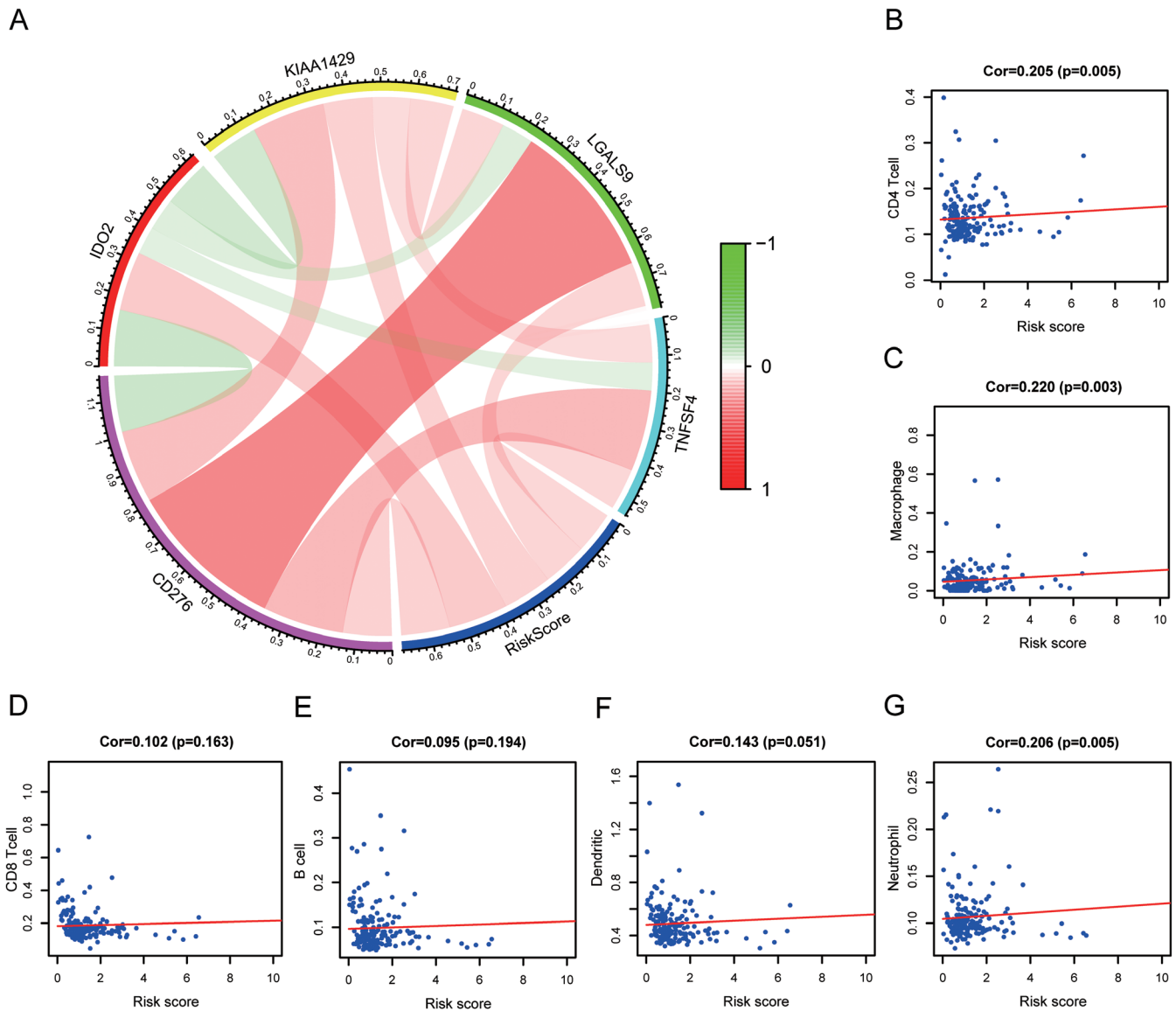


**Fig. 8. Correlation analysis between risk score and immune checkpoint gene and immune cell infiltration.** (A) Circle map of the relationships between immune checkpoint genes and integration of risk score. (B–G) Risk score for immune cell infiltration of CD4 T cells, macrophages, CD8 T cells, B cells, dendritic cells, and neutrophils.

strict screening methods on the basis of DEGs and IDEGs in TCGA database, and IGS retrieved from ImmPort. In its methodology, ssGSEA is a widely accepted algorithm to analyze statistical enrichment.<sup>30</sup> The ESTIMATE algorithm was used to calculate the stromal score, immune score and estimate score in the immune microenvironment for further immune assessment.<sup>31</sup> The Lasso algorithm, as one of the regression regularization methods, applies a Lasso Cox regression model and ensures optimal risk model, even when variables in the dataset have high dimensions and multicollinearity.<sup>32,33</sup>

As is known, binding of ligand and inhibitory receptors on immune cells will weaken the T cell mediated immune response. Antibodies against immune checkpoint proteins, such as CTLA4 or PD-1 (also called PDCD1), the first generation of antibody-based immunotherapy, has been implemented for the treatment of HCC patients. In consideration of partial immune response to these inhibitors, early

results of a recent study based on the CheckMate-040 trial (nivolumab plus ipilimumab) were obtained for patients of advanced HCC who previously received sorafenib, and demonstrated an objective response rate of 33% (95% confidence interval of 20–48) in these patients. The Food and Drug Administration has accelerated the approval of this combination therapy strategy.<sup>34</sup> Similar treatment regimens emerged for melanoma,<sup>35</sup> non-small-cell lung cancer,<sup>36</sup> and renal cell carcinoma.<sup>37</sup> Evidently, our results showed reliability and high practical utility from a clinical perspective.

Meanwhile, it is also imperative to develop novel immune therapeutic approaches. In the present study, we found *IKBKE*, *IL2RG*, *EDNRA*, and *IGHA1* to be statistically more significant with  $p < 0.2$  than *PDCD1* ( $p > 0.2$ ) among the 21 KIRGs by univariate Cox regression and multivariate Cox regression. Due to multi-step screening, we boldly defined the critical value as 0.2. *IKBKE*, a member of the nonclassical IKK family, is considered to be a potential target for

cancer therapy.<sup>38</sup> Typically, IKBKE was classified as an oncogenic effector during KRAS-induced pancreatic transformation and activated AKT signaling to promote tumorigenesis.<sup>39</sup> IKBKE-associated cytokine signaling was also shown to promote tumorigenicity of immune-driven triple-negative breast cancers.<sup>40</sup> IKBKE regulates androgen receptor levels via Hippo pathway inhibition in advanced prostate cancer.<sup>41</sup> However, the specific functions of these four factors in HCC still lack a deep understanding.

To investigate the regulatory mechanism of KIRGs, transcription factors and lncRNAs were analyzed according to their roles as crucial components of cancer regulatory networks. We identified IRLncRNAs associated with KIRGs and DETFs, and constructed a DETFs-IRLncRNAs-KIRGs regulatory network to reveal the possible functional relationship. To date, AC127024.5 has only been reported as a prognostic target for pancreatic cancer.<sup>42</sup> In HCC, we found that the NRF1-AC127024.5-IBKKE axis might be involved in the regulation of many biological processes, further underscoring its potential for clinical application. In addition, from the key IRLncRNAs-KIRGs network, we constructed a risk score model and verified the prognosis prediction efficiency, which could emphasize good compatibility and appropriate clinical applicability compared to several genes placed in a model based on only one data set. Our risk model showed more obvious discriminating power than that of tumor staging. Unfortunately, we could not find available data in the Gene Expression Omnibus and the International Cancer Genome Consortium, including KIRGs and IRLncRNAs simultaneously; thus, external validation was precluded. Ultimately, the correlation between any immune checkpoint gene and risk score indicated the current targets of immunotherapy, such as CD4 T cells and phagocytosis checkpoint immunotherapy.

Although we have identified relevant IGs, including related transcription factors and lncRNAs, there is still a long road ahead of us before these findings are able to be applied in clinical practice. This field of cancer immunotherapy also presents several obstacles and faces many challenges.<sup>43</sup> Implementation of combination therapy with immune checkpoint blockade or as an adjuvant treatment of HCC in patients will not be immediate and its potential still needs to be investigated systematically and thoroughly.

## Conclusions

In summary, our analysis results highlight the importance of IGs in the HCC microenvironment. Moreover, sufficient information on novel biomarkers, networks, and pathways further unravel the underlying molecular mechanisms in the development of HCC. Understanding the immune microenvironment signatures will be advantageous to provide persuasive justification to improve the clinical efficacy of the immunotherapy.

## Acknowledgments

We sincerely appreciate the guidance of Xinyuan Lao and Zhujun Tan of Helixlife, and the invaluable assistance of Huimei Wang, Yuanning Guo, and Liewang Qiu during the current study.

## Funding

This work was supported by the China Postdoctoral Science Foundation (grant number 2019M663445 to YC), National Natural Science Foundation of China (grant num-

ber 81602045 to JX, 81802454 to HYZ), Chongqing Basic and Frontier Research Project (grant number cstc2018jcyjAX0728 to NW), Science and Technology Planning Project of Yuzhong District of Chongqing city (grant number 20180118 to JX), and Open Research Fund Program of the Key Laboratory of Molecular Biology for Infectious Diseases, CQMU (grant number 202001 to YC).

## Conflict of interest

The authors have no conflict of interests related to this publication.

## Author contributions

Study concept and design (YC, WFH), analysis and interpretation of data (WFH, YJG), sample collection (HYZ, MXC), experimental processes and drafting of the manuscript (KZ, NW), critical revision of the manuscript for important intellectual content (YC and JX). All authors have read and approved the final manuscript.

## References

- Bray F, Ferlay J, Soerjomataram I, Siegel RL, Torre LA, Jemal A. Global cancer statistics 2018: GLOBOCAN estimates of incidence and mortality worldwide for 36 cancers in 185 countries. *CA Cancer J Clin* 2018;68:394–424. doi:10.3322/caac.21492.
- Omata M, Cheng AL, Kokudo N, Kudo M, Lee JM, Jia J, *et al*. Asia-Pacific clinical practice guidelines on the management of hepatocellular carcinoma: a 2017 update. *Hepatol Int* 2017;11:317–370. doi:10.1007/s12072-017-9799-9.
- Llovet JM, Zucman-Rossi J, Pikarsky E, Sangro B, Schwartz M, Sherman M, *et al*. Hepatocellular carcinoma. *Nat Rev Dis Primers* 2016;2:16018. doi:10.1038/nrdp.2016.18.
- Hollebecque A, Malka D, Fertié C, Ducreux M, Boige V. Systemic treatment of advanced hepatocellular carcinoma: from disillusion to new horizons. *Eur J Cancer* 2015;51:327–339. doi:10.1016/j.ejca.2014.12.005.
- Llovet JM, Ricci S, Mazzaferro V, Hilgard P, Gane E, Blanc JF, *et al*. Sorafenib in advanced hepatocellular carcinoma. *N Engl J Med* 2008;359:378–390. doi:10.1056/NEJMoa0708857.
- Cheng AL, Kang YK, Chen Z, Tsao CJ, Qin S, Kim JS, *et al*. Efficacy and safety of sorafenib in patients in the Asia-Pacific region with advanced hepatocellular carcinoma: a phase III randomised, double-blind, placebo-controlled trial. *Lancet Oncol* 2009;10:25–34. doi:10.1016/S1470-2045(08)70285-7.
- Kudo M, Finn RS, Qin S, Han KH, Ikeda K, Piscaglia F, *et al*. Lenvatinib versus sorafenib in first-line treatment of patients with unresectable hepatocellular carcinoma: a randomised phase 3 non-inferiority trial. *Lancet* 2018;391:1163–1173. doi:10.1016/S0140-6736(18)30207-1.
- Jayant K, Habib N, Huang KW, Podda M, Warwick J, Arasaradnam R. Immunological basis of genesis of hepatocellular carcinoma: Unique challenges and potential opportunities through immunomodulation. *Vaccines (Basel)* 2020;8:247. doi:10.3390/vaccines8020247.
- Zhou G, Sprengers D, Boor PPC, Doukas M, Schutz H, Manchan S, *et al*. Antibodies against immune checkpoint molecules restore functions of tumor-infiltrating T cells in hepatocellular carcinomas. *Gastroenterology* 2017;153:1107–1119.e10. doi:10.1053/j.gastro.2017.06.017.
- El-Khoueiry AB, Sangro B, Yau T, Crocenzi TS, Kudo M, Hsu C, *et al*. Nivolumab in patients with advanced hepatocellular carcinoma (CheckMate 040): an open-label, non-comparative, phase 1/2 dose escalation and expansion trial. *Lancet* 2017;389:2492–2502. doi:10.1016/S0140-6736(17)31046-2.
- Zhu AX, Finn RS, Edeline J, Cattani S, Ogasawara S, Palmer D, *et al*. Pembrolizumab in patients with advanced hepatocellular carcinoma previously treated with sorafenib (KEYNOTE-224): a non-randomised, open-label phase 2 trial. *Lancet Oncol* 2018;19:940–952. doi:10.1016/S1470-2045(18)30351-6.
- Sangro B, Gomez-Martin C, de la Mata M, Iñárraiaegui M, Garralda E, Barrera P, *et al*. A clinical trial of CTLA-4 blockade with tremelimumab in patients with hepatocellular carcinoma and chronic hepatitis C. *J Hepatol* 2013;59:81–88. doi:10.1016/j.jhep.2013.02.022.
- Yau T, Kang YK, Kim TY, El-Khoueiry AB, Santoro A, Sangro B, *et al*. Nivolumab (NIVO) + ipilimumab (IPI) combination therapy in patients (pts) with advanced hepatocellular carcinoma (aHCC): Results from CheckMate 040. *J Clin Oncol* 2019;37:4012. doi:10.1200/JCO.2019.37.15\_suppl.4012.
- Finn RS, Ryoo BY, Merle P, Kudo M, Bouattour M, Lim HY, *et al*. Pembrolizumab as second-line therapy in patients with advanced hepatocellular carcinoma in KEYNOTE-240: A randomized, double-blind, phase III trial. *J*

- Clin Oncol 2020;38:193–202. doi:10.1200/JCO.19.01307.
- [15] Hutter C, Zenklusen JC. The cancer genome atlas: Creating lasting value beyond its data. *Cell* 2018;173:283–285. doi:10.1016/j.cell.2018.03.042.
- [16] Bhattacharya S, Andorf S, Gomes L, Dunn P, Schaefer H, Pontius J, *et al*. ImmPort: disseminating data to the public for the future of immunology. *Immunol Res* 2014;58:234–239. doi:10.1007/s12026-014-8516-1.
- [17] Subramanian A, Tamayo P, Mootha VK, Mukherjee S, Ebert BL, Gillette MA, *et al*. Gene set enrichment analysis: a knowledge-based approach for interpreting genome-wide expression profiles. *Proc Natl Acad Sci U S A* 2005;102:15545–15550. doi:10.1073/pnas.0506580102.
- [18] Godec J, Tan Y, Liberzon A, Tamayo P, Bhattacharya S, Butte AJ, *et al*. Compendium of immune signatures identifies conserved and species-specific biology in response to inflammation. *Immunity* 2016;44:194–206. doi:10.1016/j.immuni.2015.12.006.
- [19] Li T, Fu J, Zeng Z, Cohen D, Li J, Chen Q, *et al*. TIMER2.0 for analysis of tumor-infiltrating immune cells. *Nucleic Acids Res* 2020;48:W509–W514. doi:10.1093/nar/gkaa407.
- [20] Verhaak RG, Tamayo P, Yang JY, Hubbard D, Zhang H, Creighton CJ, *et al*. Prognostically relevant gene signatures of high-grade serous ovarian carcinoma. *J Clin Invest* 2013;123:517–525. doi:10.1172/JCI65833.
- [21] Ritchie ME, Phipson B, Wu D, Hu Y, Law CW, Shi W, *et al*. limma powers differential expression analyses for RNA-sequencing and microarray studies. *Nucleic Acids Res* 2015;43:e47. doi:10.1093/nar/gkv007.
- [22] Langfelder P, Horvath S. WGCNA: an R package for weighted correlation network analysis. *BMC Bioinformatics* 2008;9:559. doi:10.1186/1471-2105-9-559.
- [23] Liu CJ, Hu FF, Xia MX, Han L, Zhang Q, Guo AY. GSCALite: a web server for gene set cancer analysis. *Bioinformatics* 2018;34:3771–3772. doi:10.1093/bioinformatics/bty411.
- [24] Wang S, Sun H, Ma J, Zang C, Wang C, Wang J, *et al*. Target analysis by integration of transcriptome and ChIP-seq data with BETA. *Nat Protoc* 2013;8:2502–2515. doi:10.1038/nprot.2013.150.
- [25] Zhou Y, Zhou B, Pache L, Chang M, Khodabakhshi AH, Tanaseichuk O, *et al*. Metascape provides a biologist-oriented resource for the analysis of systems-level datasets. *Nat Commun* 2019;10:1523. doi:10.1038/s41467-019-09234-6.
- [26] Szklarczyk D, Gable AL, Lyon D, Junge A, Wyder S, Huerta-Cepas J, *et al*. STRING v11: protein-protein association networks with increased coverage, supporting functional discovery in genome-wide experimental datasets. *Nucleic Acids Res* 2019;47:D607–D613. doi:10.1093/nar/gky1131.
- [27] Yang W, Soares J, Greninger P, Edelman EJ, Lightfoot H, Forbes S, *et al*. Genomics of Drug Sensitivity in Cancer (GDSC): a resource for therapeutic biomarker discovery in cancer cells. *Nucleic Acids Res* 2013;41:D955–D961. doi:10.1093/nar/gks1111.
- [28] Seashore-Ludlow B, Rees MG, Cheah JH, Cokol M, Price EV, Coletti ME, *et al*. Harnessing connectivity in a large-scale small-molecule sensitivity dataset. *Cancer Discov* 2015;5:1210–1223. doi:10.1158/2159-8290.CD-15-0235.
- [29] Binnewies M, Roberts EW, Kersten K, Chan V, Fearon DF, Merad M, *et al*. Understanding the tumor immune microenvironment (TIME) for effective therapy. *Nat Med* 2018;24:541–550. doi:10.1038/s41591-018-0014-x.
- [30] Barbie DA, Tamayo P, Boehm JS, Kim SY, Moody SE, Dunn IF, *et al*. Systematic RNA interference reveals that oncogenic KRAS-driven cancers require TBK1. *Nature* 2009;462:108–112. doi:10.1038/nature08460.
- [31] Yoshihara K, Shahmoradgoli M, Martínez E, Vegesna R, Kim H, Torres-García W, *et al*. Inferring tumour purity and stromal and immune cell admixture from expression data. *Nat Commun* 2013;4:2612. doi:10.1038/ncomms3612.
- [32] Atabaki-Pasdar N, Ohlsson M, Viñuela A, Frau F, Pomares-Millan H, Haid M, *et al*. Predicting and elucidating the etiology of fatty liver disease: A machine learning modeling and validation study in the IMI DIRECT cohorts. *PLoS Med* 2020;17:e1003149. doi:10.1371/journal.pmed.1003149.
- [33] Lee BP, Vittinghoff E, Hsu C, Han H, Therapondos G, Fix OK, *et al*. Predicting low risk for sustained alcohol use after early liver transplant for acute alcoholic hepatitis: The sustained alcohol use post-liver transplant score. *Hepatology* 2019;69:1477–1487. doi:10.1002/hep.30478.
- [34] Wright K. FDA approves nivolumab plus ipilimumab for the treatment of advanced HCC. *Oncology (Williston Park)* 2020;34:693606.
- [35] Zimmer L, Livingstone E, Hassel JC, Fluck M, Eigentler T, Loqui C, *et al*. Adjuvant nivolumab plus ipilimumab or nivolumab monotherapy versus placebo in patients with resected stage IV melanoma with no evidence of disease (IMMUNED): a randomised, double-blind, placebo-controlled, phase 2 trial. *Lancet* 2020;395:1558–1568. doi:10.1016/S0140-6736(20)30417-7.
- [36] Hellmann MD, Paz-Ares L, Bernabe Caro R, Zurawski B, Kim SW, Carcereny Costa E, *et al*. Nivolumab plus ipilimumab in advanced non-small-cell lung cancer. *N Engl J Med* 2019;381:2020–2031. doi:10.1056/NEJMoa1910231.
- [37] Tomita Y, Kondo T, Kimura G, Inoue T, Wakumoto Y, Yao M, *et al*. Nivolumab plus ipilimumab versus sunitinib in previously untreated advanced renal-cell carcinoma: analysis of Japanese patients in CheckMate 214 with extended follow-up. *Jpn J Clin Oncol* 2020;50:12–19. doi:10.1093/jjco/hyz132.
- [38] Yin M, Wang X, Lu J. Advances in IKBKE as a potential target for cancer therapy. *Cancer Med* 2020;9:247–258. doi:10.1002/cam4.2678.
- [39] Rajurkar M, Dang K, Fernandez-Barrena MG, Liu X, Fernandez-Zapico ME, Lewis BC, *et al*. IKBKE is required during KRAS-induced pancreatic tumorigenesis. *Cancer Res* 2017;77:320–329. doi:10.1158/0008-5472.CAN-15-1684.
- [40] Barbie TU, Alexe G, Aref AR, Li S, Zhu Z, Zhang X, *et al*. Targeting an IKBKE cytokine network impairs triple-negative breast cancer growth. *J Clin Invest* 2014;124:5411–5423. doi:10.1172/JCI75661.
- [41] Bainbridge A, Walker S, Smith J, Patterson K, Dutt A, Ng YM, *et al*. IKBKE activity enhances AR levels in advanced prostate cancer via modulation of the Hippo pathway. *Nucleic Acids Res* 2020;48:5366–5382. doi:10.1093/nar/gkaa271.
- [42] Wei C, Liang Q, Li X, Li H, Liu Y, Huang X, *et al*. Bioinformatics profiling utilized a nine immune-related long noncoding RNA signature as a prognostic target for pancreatic cancer. *J Cell Biochem* 2019;120:14916–14927. doi:10.1002/jcb.28754.
- [43] Hegde PS, Chen DS. Top 10 challenges in cancer immunotherapy. *Immunity* 2020;52:17–35. doi:10.1016/j.immuni.2019.12.011.